12WCEE 2000

0454

MULTI-DIRECTIONAL LOADING TEST FOR RC SEISMIC SHEAR WALLS

Atsushi HABASAKI[1], Yoshio KITADA[2], Takao NISHIKAWA[3], Katsuki TAKIGUCHI[4] And Haruhiko TORITA[5]

SUMMARY

Nuclear Power Engineering Corporation (NUPEC) has been conducting a project entitled "Model Tests of Multi-axis Loading on RC Shear Walls" to clarify the elasto-plastic characteristics of an RC box type seismic shear wall, and to develop a method of evaluating restoring force characteristics under multi-directional seismic loads. This paper presents a summary of the diagonal loading test which was performed as a part of the project, and proposes an evaluation method for both shear and bending components of restoring force characteristics of an RC box type seismic shear wall subjected to diagonal load. Through comparing test results and calculated results of the proposed evaluation method, the applicability of the proposed method is demonstrated.

INTRODUCTION

In the current seismic design of nuclear power plant (NPP) buildings in Japan, seismic design loads in the two orthogonal, horizontal directions are obtained independently from seismic response analyses, whereas actual seismic forces jolt the buildings in the three directions simultaneously. Therefore, it is important to upgrade the seismic design methodology for NPP buildings from the viewpoint of multi-directional earthquake excitation. Nuclear Power Engineering Corporation (NUPEC) has therefore been conducting a project entitled “Model Tests of Multi-axis Loading on RC Shear Walls” since 1994. The objectives are to clarify the effects of multi-directional input forces on the ultimate strength of reinforced concrete (RC) seismic shear wall, which is a main earthquake resistance element in NPP buildings, and to predict nonlinear behavior of an RC seismic shear wall under multi-directional loading. The project is commissioned by the Ministry of International Trade and Industry (MITI) of Japan. In the test, we accumulated static and dynamic test data by multi-directional loading tests firstly, and developed the evaluation method of restoring force characteristics of an RC seismic shear wall subjected to multi-directional loads. This paper describes a summary of the diagonal loading tests which was carried out as a part of the project, and proposes an evaluation method for the restoring force characteristics of an RC box type seismic shear wall subjected to diagonal load.

TEST CONDITIONS

Test Specimens

Figure 1 shows the typical shapes and dimensions of the test specimens of box type shear walls. Table 1 gives specifications of all specimens and test parameters for the diagonal loading test. As for the test parameters, shear span ratios (M/QD) of 0.6, 0.8 and 1.0 for RC box type shear walls were taken based on a survey of actual NPP reactor buildings in Japan. Horizontal loading angles (θ) of 0, 26.6, and 45 degrees (°) were also taken. In case of $\theta = 26.6°$, the ratio of effective wall length working as web and flange walls becomes 1 : 0.5. In all specimens, reinforcing bars, whose yield strength was 345N/mm^2, were deployed in the vertical and transverse directions with double-fold in 70 mm pitch, which were equivalent to 1.2% of reinforcement ratio. The walls were made up of concrete of pea gravel to have design strength of 30 MPa. Concrete strength of each specimen during the test is shown in Table 1.

[1] *Seismic Engineering Center, Nuclear Power Engineering Corporation, Tokyo, Japan, Email: habasakit@nupec.or.jp*
[2] *Seismic Engineering Center, Nuclear Power Engineering Corporation, Tokyo, Japan, Dr. Eng., Email: kitada@nupec.or.jp*
[3] *Department of Architecture, Tokyo Metropolitan University, Tokyo, Japan, Dr. Eng., Email:tanishi@arch.metro-u.ac.jp*
[4] *Dept of Mechanical and Environmental Information, Tokyo Institute of Technology, Japan, Email:ktakiguc@o.cc.titech.ac.jp*
[5] *Engineering Division, Shimizu Corporation, Tokyo, Japan, Email: tori@eng.shimz.co.jp*

Loading Plan

The load applied to the specimen was controlled with monitored force and displacement in the test to prevent torsional deformation. Figure 2 shows the loading cycle. Lateral forces were increased gradually until specific horizontal deformation reached 0.5, 1.0, 2.0, 4.0, 6.0, and 8.0×10^{-3} radian twice both in the positive and negative directions. The final loading was carried out at the ultimate point of the positive direction. Figure 3 shows loading apparatus setup example used in the test. The axial stress is applied using an actuator to the loading slab on the specimen. Constant axial stress of σ_V =1.47MPa, which was decided by survey of actual reactor buildings, was applied. Photo-1 shows a schematic view of a specimen and loading apparatus.

TEST RESULTS

Typical test results are shown in Figure 4 and Table 2. Figure 4 shows the relationship between load and overall deformation of SD-08 series, and Table 2 gives the summary of all test results.

Crack Pattern

Figure 5 shows the final crack pattern of the SD-08 series specimens. In case of $\theta = 0°$, shear sliding failure occurred around the lower portion of faces C and A during the positive and negative loading of 8×10^{-3} radian. After reaching that deformation, strength decreased rapidly. Also, in case of $\theta = 26.6°$, the same failure occurred around the lower portion of face C. In case of $\theta = 45°$, shear sliding failure occurred around the lower portions of faces A and D, and failure occurred around the lower portions of faces B and C simultaneously. It should be noted that despite this damage, the strength of the walls decreased gradually. Similarly, different crack patterns were generated corresponding to different loading angles in other test specimens having other shear span ratios.

Envelope Curves

Figure 6 shows a comparison of envelope curves between load and overall deformation. For all specimens of $\theta = 26.6°$ and 45° cases, the maximum load and its overall deformation became larger than those of $\theta = 0°$.

Deformation Components

Using the displacement data, overall deformation was separated into shear, bending, and rotational components. Figure 7 shows a typical share of the deformation components at the peak of the initial loading cycle the SD-08 series. It was found that the ratio of each deformation component was not affected by the loading angle. The ratios of shear deformation to total deformation decreased with increments of M/QD values. The values were about 80 to 85% for M/QD=0.6 specimens, 70 to 75% for M/QD=0.8 and 60 to 70% for M/QD=1.0 specimens.

EVALUATION METHOD FOR RESTORING FORCE CHARACTERISTICS

Evaluation Method Proposal

The present evaluation methodology of restoring force characteristics of RC seismic shear walls for NPP buildings was established in Japan in the "Technical guidelines for aseismic design of nuclear power plants" issued by the Japan Electric Association (JEAG)" (hereinafter JEAG model) [2]. However, the JEAG model had been constructed mainly based on the shear wall test data of a loading angle of 0° , and the effects of different loading angles had not been explicitly taken into account. Therefore, we developed an evaluation method of restoring force characteristics of an RC seismic shear wall by referring to the JEAG model and taking into account the effect of loading angles on the restoring force characteristics to predict elasto-plastic behaviors of the wall properly in multi-directional loading. Since the JEAG model was not established based on SI units, conventional units system is used in the following process.

(1) Shear component
In the JEAG model, skeleton curve for shear component is idealized with a tri-linear model. In diagonal loading, we propose the quarto-linear model whose four turning points are determined in the following manner.
a. First turning point (τ_1 , γ_1)
The shear stress τ_1 of the JEAG model was determined from average shear stress on the wall at the time the initial shear crack is generated at the center of the specimen wall. The existing data obtained by in-plane shear force loading test indicate that the shear cracks reduce shear stiffness of the RC shear walls. It is supposed that the reduction rate varies with the change of loading angle. In order to understand the effect, the loads at the time the initial shear crack was generated, are compared with those calculated using the JEAG model and shown in

Table 3. It is found that the test results (Qcr) are smaller than the calculated results (cQcr). The reason is that τ_1 is determined from shear stress at the time when the initial crack was generated, not the time when the shear crack was generated at the center of the wall. In the test results, there are no uniform trends related to the loading angle. Based on the results, it is concluded that τ_1 could be determined to be the same value with the JEAG model despite the different loading angles. Shear strain γ_1 could also be calculated by the following equation, in the same manner as the JEAG model;

$$\gamma_1 = \tau_1 / G \quad (1).$$

b. Second turning point (τ_2 , γ_2)

The values of τ_2 and γ_2 in the JEAG model were calculated using the value of γ_1 and τ_1 as;

$$\tau_2 = 1.35 \times \tau_1 \quad (2)$$

$$\gamma_2 = 3 \times \gamma_1 \quad (3).$$

The relationships were obtained by fitting the equations to the existing test data. Because there is no specific contradiction for using the equations for diagonal loading, we will use the equations in our calculation.

c. Third turning point (τ_3 , γ_3)

The maximum shear stress of τ_3 in the JEAG model was expressed by combining the strength of reinforcing bars and concrete. The contribution of reinforcing bars to the maximum stress is calculated using the reinforcing ratio and axial stress of the wall, and the contribution of concrete is calculated using the concrete strength and shear span ratio. When box type seismic shear wall is subjected to diagonal load, the effective cross section width (d') to the loading axis becomes larger than the case of $\theta = 0°$. Shear span ratio with d' (M/Qd') becomes smaller in accordance with loading angle. In case of diagonal loading, we decide to evaluate τ_3 based on the JEAG model by replacing d and M/Qd by d' and M/Qd' respectively as ;

$$d' = d \times \sqrt{2} \times \cos(45 - \theta) \quad (4)$$

$$M/Qd' = (M/Qd) / \{\sqrt{2} \times \cos(45 - \theta)\} \quad (5)$$

where, d : cross section width of $\theta = 0°$

d' : effective cross section width corresponding to the loading angle.

Figure 8 shows the maximum shear forces applied to the two horizontal orthogonal directions. In the figure, both test and calculated maximum shear forces are normalized by the maximum shear forces obtained from the data of $\theta = 0°$ cases. The calculated results agree well with the test results. In general, the maximum shear forces seemed to be hardly affected by the angle of applied load and shear span ratio. However, both test and calculated results are plotted slightly outside of the arc which representing the combination of two orthogonal horizontal loads. The fact indicates that maximum load for overall specimen increases a little bit for the case of diagonal loading with the increment of the loading angle. Values of shear strain at the maximum shear stress, are not affected by loading angle and shear span ratio. After that point, the shear strain increases with the increment of the loading angle despite the fact that the shear stress keeps constant. Referring to this test results and considering current practice, we decide that the value of γ_3 should be 4×10^{-3} or the same value as the JEAG model.

d. Ultimate point (τ_u , γ_u)

In diagonal loading, stiffness reduction was not observed after reaching the maximum shear force (third turning point), nevertheless deformation under the maximum force increased with the increment of the loading angle. Thus, the maximum shear stress was retained after the third turning point until the value of τ reached the ultimate shear stress τ_u . It was reported that the ultimate shear strain of cylindrical test specimens tended to be greater than that of box type test specimens [3]. The reason may be that the stress in each wall is transferred smoothly in a cylindrical seismic shear wall compared with a box type seismic shear wall. Figure 9 shows the relationship between loading angle and the maximum shear strain at the point of maximum shear stress generated. In this figure, the data of $\theta = 90°$ and $63.4°$ are plotted by assuming that they are equivalent with those of $\theta = 0°$ and $23.6°$. The ultimate shear strain increases, with some variance, with the increment of the loading angle from $0°$ to $45°$. Although the accuracy of separated deformation components decreases near the ultimate condition, the ultimate shear strain increases apparently with the increment in the loading angle.

Based on the test results, ultimate shear strain γ_u of proposed method is expanded from γ_3 . The value is proposed as a function of loading angle (θ) as follows ;

$$\gamma_u = \alpha \times \gamma_3 = \alpha \times 4 \times 10^{-3} \quad (6)$$

where, $\alpha = 1/\cos\theta$: $0° < \theta \leq 45°$

$\alpha = 1/\sin\theta$: $45° < \theta \leq 90°$.

Figure 10 shows the maximum shear strain at the maximum shear stress determined from the test data. The data are plotted on the axis of two horizontal orthogonal directions. Equation (6) shows the squared shape in this figure. Each test result is equivalent or larger than the value of γ_u obtained by Equation (6). Thus, the results demonstrate the adequacy of the proposed method with some margin.

(2) Bending component

When we evaluate bending stiffness of a box type RC seismic shear wall under the diagonal loading accurately,

it is necessary to use a detailed model where the cross section of the wall is divided into small pieces in the direction perpendicular to the loading axis. However, this method is very complicated and impractical for use in design analyses. Therefore, we decide to evaluate the skeleton curve for bending component after the JEAG model (M-ϕ relationship). The area used is determined by projecting the cross section to the axis perpendicular to the loading axis. Although the method has a weak point in the accuracy in evaluating the bending stiffness of a box type RC seismic shear wall, it is still applicable because the bending component share is very small as compared with the shear component as shown in Figure 7.

Evaluation Method Applicability

Skeleton curves obtained from the proposed evaluation method are compared with the test results. The evaluation of rotational deformation (R_θ) is very difficult particularly for diagonal loading, because reinforcing bars were pulled out from the base mat. Therefore, we defined each deformation component as follow ; R_T : overall deformation obtained from test result, $R_T - R_\theta$ (R_T minus R_θ) : overall deformation, R_S : shear deformation, and $R_T - R_S - R_\theta$: bending deformation. Figure 11 shows the comparison of test and calculated results of the relationship between each deformation component and shear force. In the shear deformation component, calculated first, second and ultimate points agree well with the test results, while in the bending component, calculated stiffness becomes greater than the test results. As for the reasons, it is pointed out that all flange area are applied in the proposed method using the JEAG model, the effect of out-of plane bending moment is eliminated in this evaluation, and the Navier's assumption of plane holding for the bending load may not be applicable in diagonal loading. However, in the NPP buildings, shear deformation is dominant and the effect of bending components is relatively small. Consequently, the restoring force characteristics on the overall deformations correspond well and the applicability of the evaluation method is confirmed. Judging from above mentioned results, the proposed method can evaluate both shear and bending components restoring force characteristics of an RC box type seismic shear wall subjected to diagonal loading. However, applicability of the M-ϕ relationship of the proposed method tended to be inferior to that of the τ-γ relationship. It will be necessary to make an effort to improve the accuracy of the M-ϕ relationship. The Proposed evaluation method of restoring force characteristics is summarized in Table 4.

CONCLUSIONS

(1) The diagonal loading test was conducted to understand the elasto-plastic characteristics of an RC box type seismic shear wall as a part of "Model tests of multi-axes loading on RC shear walls" project.
(2) The maximum load and overall deformation at the maximum load were affected by loading angle. The data of all specimens of $\theta = 26.6°$ and $45°$ indicated that the maximum load and the overall deformation at the maximum load became larger than those of $\theta = 0°$.
(3) Different crack patterns were observed in different loading angles. The proportion of shear deformation to overall deformation decreased with the increment of shear span ratio. The proportion became almost constant despite of the difference of the loading angles.
(4) The evaluation method of the restoring force characteristics for an RC box type seismic shear wall subjected to diagonal load was proposed based on the test results.
(5) The comparison between test and calculated results demonstrated the adequacy of the proposed evaluation method both in shear and bending component restoring force characteristics of an RC box type seismic shear wall subjected to diagonal load.

ACKNOWLEDGMENTS

This work was performed by NUPEC as a part of the "Model Tests of Multi-axis Loading on RC Shear Walls" project commissioned by the Ministry of International Trade and Industry (MITI) of Japan. Technical issues have been discussed in the advisory committee on the project established within NUPEC (Chairperson : Professor Dr. T. Nishikawa). The authors wish to express their thanks to all the members of committee for their valuable suggestions and cooperation.

REFERENCES

1. Habasaki, A., Kitada, Y., Nishikawa, T., Takiguchi, K., Torita, H. (1999), "Multi-Axial Loading Test for RC Wall of Reactor Building", *SMiRT-15, (submitted),* Seoul.
2. Japan Electric Association, *Technical Guidelines for Aseismic Design of Nuclear Power Plants,* JEAG 4601-1991 Supplement, 1991.
3. Kai, Y., Takeda, M., Shohara, R., Ohtani, K., Akino, K. (1993), "Uncertainty of restoring force characteristics of shear walls and its effect on seismic response", *SMiRT-12*,K09/2, Stuttgart, pp.253-258.
4. Nuclear Power Engineering Corporation, *Model Tests of Multi-Axis Loading on RC Shear Walls*, Report for fiscal 1994-1998.

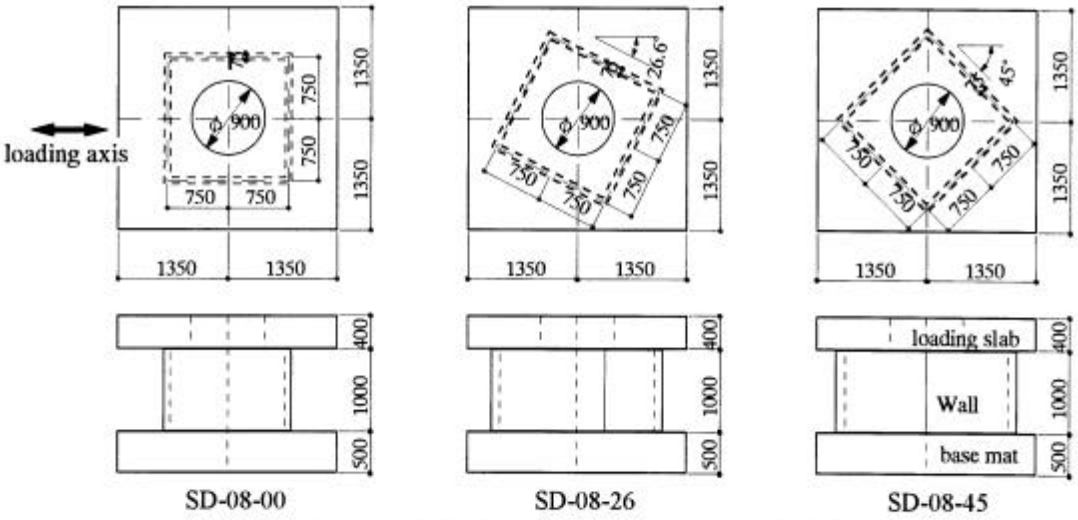

Fig.1 Shapes and dimensions of the test specimens (SD-08 series)

Table 1 Test specimens

Specimens code	Shear span ratio M/QD	Loading angle θ (°)	Concrete strength (MPa)
SD-06-00	0.6	0	30.7
SD-06-26		26.6	29.2
SD-06-45		45	33.2
SD-08-00	0.8	0	34.9
SD-08-26		26.6	34.8
SD-08-45		45	37.4
SD-10-00	1.0	0	37.8
SD-10-45		45	37.2

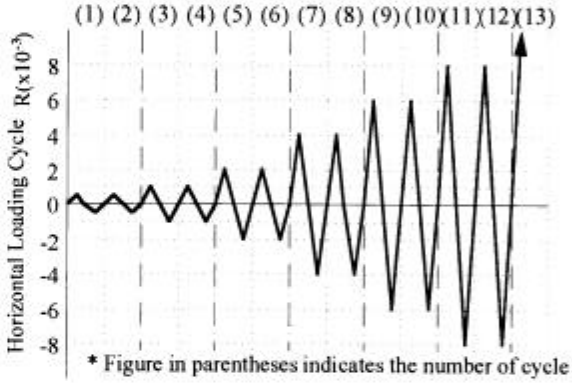

Fig. 2 Loading Cycle

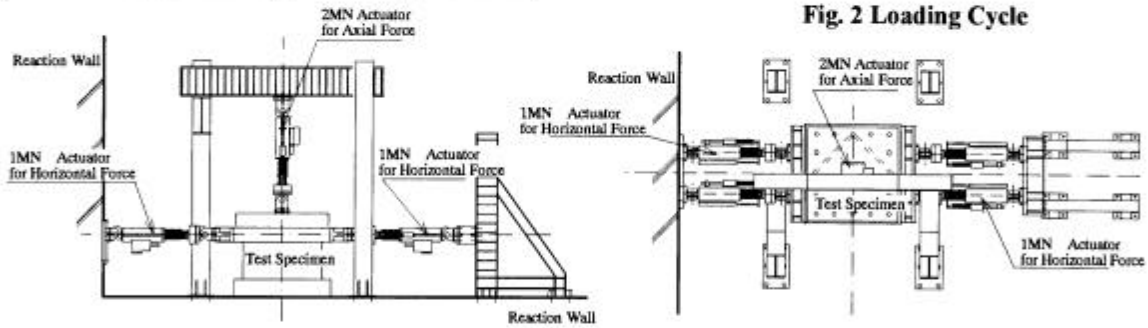

Fig.3 Loading apparatus

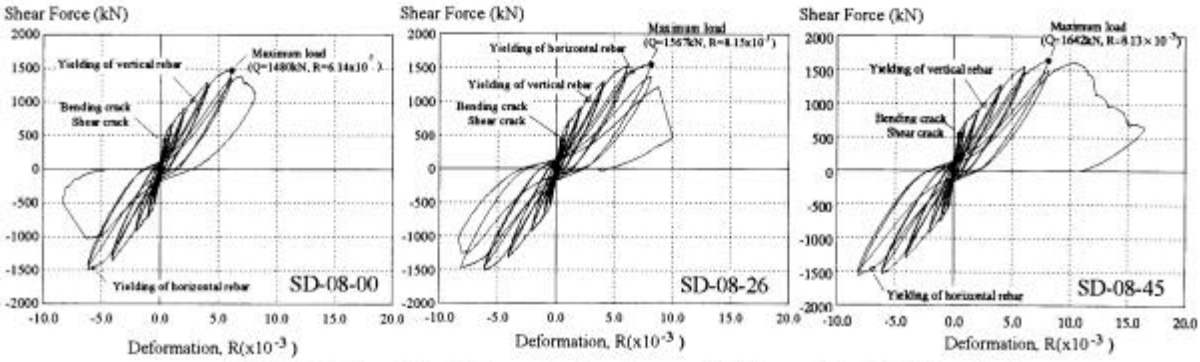

Fig.4 Relationships between load and overall deformation (SD-08 series)

Table 2 Summary of test results

Specimens	Initial stiffness	Bending crack		Shear crack		Yield of vertical rebar		Yield of horizontal rebar		Maximum load	
	K0 (MN/mm)	Q (KN)	R ($\times 10^{-3}$)	Q (KN)	R ($\times 10^{-3}$)	Q (KN)	R ($\times 10^{-3}$)	Q (KN)	R ($\times 10^{-3}$)	Q (KN)	R ($\times 10^{-3}$)
SD-06-00	2.01	517	0.53	442	0.40	1376	3.81	1527	8.11	1686	6.11
SD-06-26	1.80	330	0.20	488	0.33	1206	2.68	1701	6.97	1794	6.31
SD-06-45	1.91	399	0.34	399	0.34	1213	3.48	1659	11.25	1835	10.81
SD-08-00	1.50	437	0.36	437	0.36	1044	2.84	-1461	-5.65	1480	6.14
SD-08-26	1.48	448	0.43	448	0.43	1036	2.72	1448	6.53	1567	8.15
SD-08-45	1.61	560	0.51	532	0.50	985	2.55	-1454	-6.90	1642	8.13
SD-10-00	0.95	389	0.44	299	0.30	932	2.82	1141	6.27	1231	6.00
SD-10-45	1.17	349	0.33	407	0.42	811	2.34	1305	7.41	1334	8.01

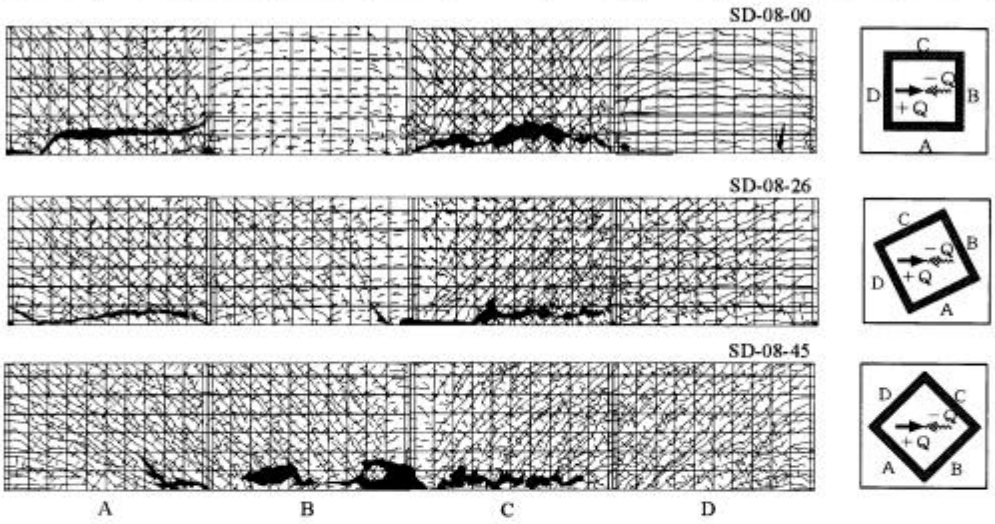

Fig.5 Final crack patterns (SD-08 series)

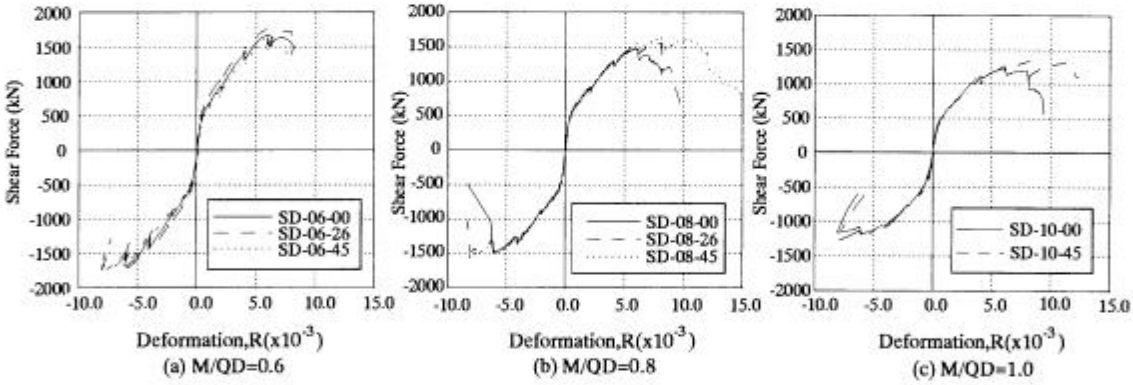

Fig. 6 Comparison of the envelope curves between load and overall deformation

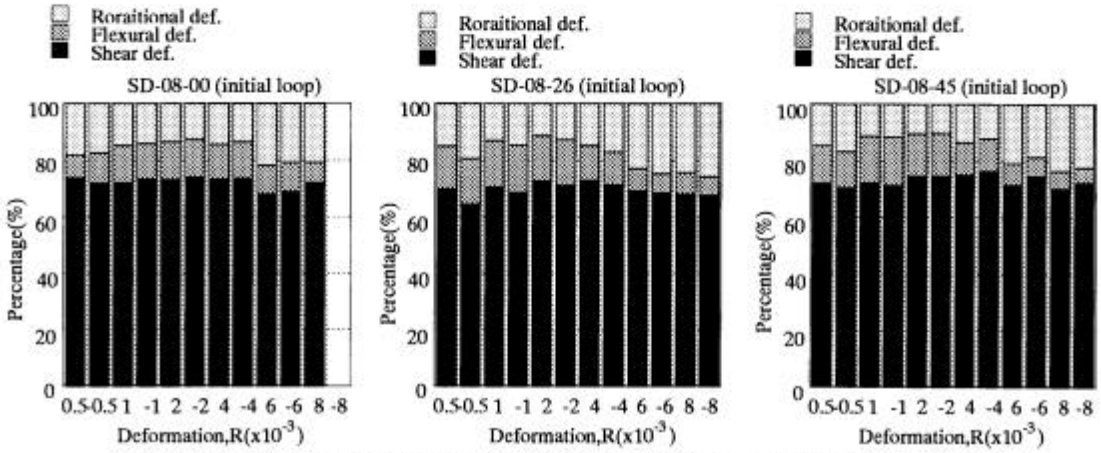

Fig. 7 Proportion of deformation components at the cycle peak (SD-08 series)

Table 3 Summary of test results

Specimens	θ (°)	Fc (kgf/cm2)	Qcr(tf) test	cQcr(tf) calculation	test / calculation	Qcr'= Qcr/√Fc	Qcr' / Qcr,0'
SD-06-00	0	313	45.1	54.1	0.83	2.55	1.00
SD-06-26	26.6	298	49.8	53.1	0.94	2.88	1.13
SD-06-45	45	339	40.7	55.8	0.73	2.21	0.87
SD-08-00	0	356	44.6	56.9	0.78	2.36	1.00
SD-08-26	26.6	355	45.7	56.8	0.80	2.43	1.03
SD-08-45	45	381	54.2	58.4	0.93	2.77	1.17
SD-10-00	0	385	30.5	58.6	0.52	1.55	1.00
SD-10-45	45	379	41.5	58.3	0.71	2.13	1.37

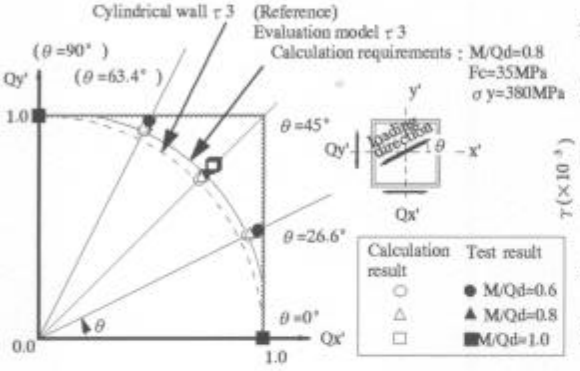

Fig.8 Maximum shear force on the axis of horizontal two directions

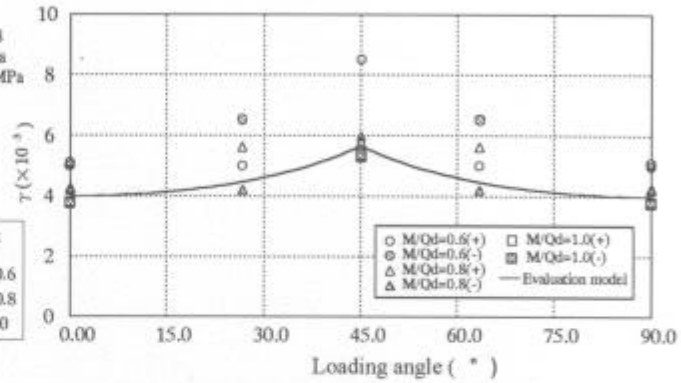

Fig.9 Relationship between loading angle and maximum shear strain

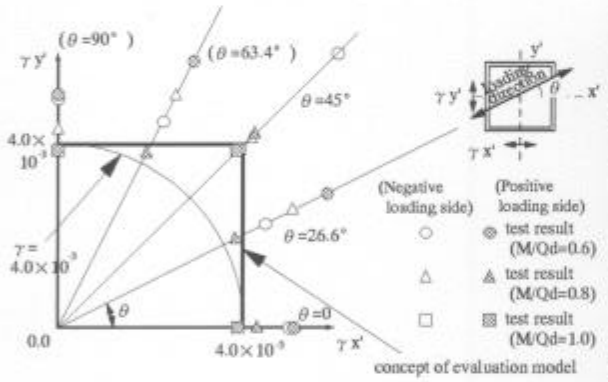

Fig.10 Maximum shear strain on the axis of horizontal two directions

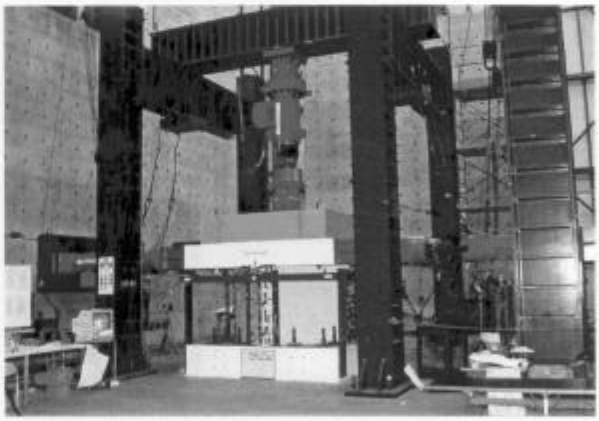

Photo.1 Test specimen installed in the loading apparatus

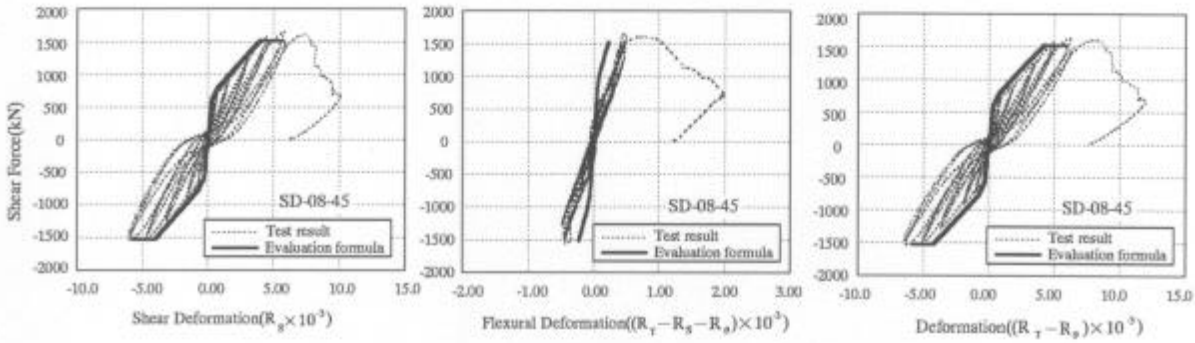

(a) Shear Component **(b) Bending Component** **(c) Overall Deformation**

Fig.11 Comparison of test and calculated result

Table 4 Proposed Evaluation Method (skeleton curve)

■ Relationships between τ and γ

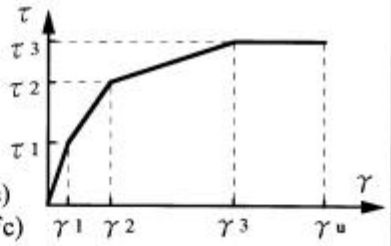

(1) $\tau_1 \cdot \gamma_1$ $\tau_1=\sqrt{(\sqrt{Fc}(\sqrt{Fc}+\sigma_v))}$

$\gamma_1=\tau_1/G$

(2) $\tau_2 \cdot \gamma_2$ $\tau_2=1.35 \cdot \tau_1$

$\gamma_2=3 \cdot \gamma_1$

(3) $\tau_3 \cdot \gamma_3$ $\tau_3=\{1-\tau_s/(4.5\sqrt{Fc})\}\tau_o+\tau_s$ $(\tau_s \leqq 4.5\sqrt{Fc})$

$=4.5\sqrt{Fc}$ $(\tau_s > 4.5\sqrt{Fc})$

$\gamma_3=4.0\times10^{-3}$

$\tau_o=(3-1.8M/Qd')\sqrt{Fc}$ $(M/Qd' > 1$ then $M/Qd'=1)$

$\tau_s=(pv+ph)s\sigma_y/2+(\sigma_v+\sigma_h)/2$

(4) γ_u $\gamma_u=\alpha \times \gamma_3$

$\alpha=1/\cos\theta$ then $0° \leqq \theta < 45°$

$\alpha=1/\sin\theta$ then $45° \leqq \theta < 90°$

Shearing area of cross-section is not depended on the loading angle that it supposed to As=Aw/2 uniformly.

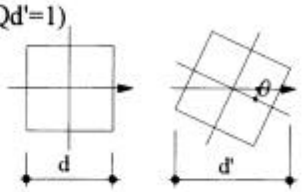

Depth of the cross section

■ Relationships between M and ϕ

The following simplified section model is assumed.

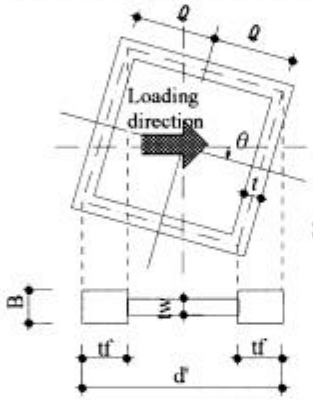

$B=t/\cos\theta + t/\sin\theta$

$d'=2Q\sqrt{2}\cos(45-\theta)$

$tw=2t/\cos\theta$

$tf=Q\sqrt{2}(\cos(45-\theta)-\sin(45-\theta))$

Simplified section model

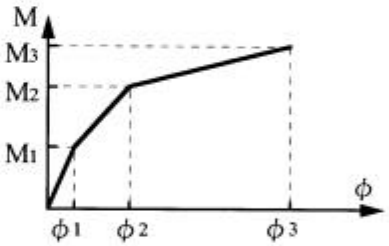

(1) $M_1 \cdot \phi_1$ $M_1=Ze'(1.2\sqrt{Fc}+\sigma_v)$

$\phi_1=M_1/(cE \cdot Ie')$

(2) $M_2 \cdot \phi_2$ $M_2=My$

M_2, ϕ_2 are taken as the flexural moment and curvature when the tensile reinforcement yield.

(3) $M_3 \cdot \phi_3$ $M_3=Mu$ (total plastic formula)

M_3 is calculated using the total plastic formula.

$\phi_3=0.004/Xnu$ then $\phi_3 < 20\phi_2$

$\phi_3=20\phi_2$ then $\phi_3 \geqq 20\phi_2$

ϕ_3 is the curvature corresponding to M_3 calculated as above.

Symbols in the table as follows;

Fc : Strength of concrete (kgf/cm²)
G : Shear modulus of elasticity concrete (kgf/cm²)
pv,ph : Longitudinal reinforcing bar ratio
transverse reinforcing bar ratio (%)
σ_v, σ_h : Vertical, horizontal axial stress (kgf/cm²)
$s\sigma_y$: Yield stress of reinforcement (kgf/cm²)
d' : Depth of the cross section for loading axial
$d'=d\sqrt{2}\cos(45-\theta)$
M/Qd' : The shear span ratio for loading direction to be considered
$M/Qd'=(M/Qd)/\sqrt{2}\cos(45-\theta)$
Ze' : Simplified effective section modulds (cm³)
cE : Young's modulus of concrete (kgf/cm²)
Ie' : Simplified effective second moment of inertia (cm⁴)
My : Moment of tension reinforcement when yielding (kgf·cm)
ϕ_y : Curvature of tension reinforcement when yielding
Mu : Plastic moment (kgf·cm)
Xnu : The distance from the extreme compression fiber to the centroid of the full-plastic cross-section (cm)